JOURNAL OF MATERIALS SCIENCE 26 (1991) 2677–2684

Transversal compression fracture of unidirectional fibre-reinforced plastics

S. L. BAZHENOV, V. V. KOZEY
Institute of Chemical Physics, Academy of Sciences of the USSR, Kosygin Str. 4, 117 977 Moscow, USSR

Transversal compression failure is a result of shear in a plane oriented at some angle to the load axis. Shear crack appears initially at an angle of 35° to 45° to the loading axis. In glass and carbon fibre-reinforced plastics the crack later turns along the load direction. As the failure mechanism at transversal compression and shear is the same, transversal compression may be used to measure composite shear strength. In aramid fibre-reinforced plastics shear yield lines appear exactly at an angle of 45° to the loading direction. Each shear line consists of a number of perpendicular micro lines of ~ 10 μm length. The directions of the yield lines and shear macro cracks do not coincide. Transversal compression strength practically does not depend on fibre content, V_f. Normalized shear and transversal compression strengths plotted against square root of pore content are described by a single straight line.

1. Introduction

Although fibre-reinforced plastics (FRP) are widely used as load-bearing materials, their compression fracture in the direction transverse to the fibres has not been carefully investigated, because of the relatively rare use of composites in transversely loaded parts. Nevertheless, in some cases, bearing properties of a composite may be limited by its transversal characteristics. An example is the use of CFRP in motor brushes where it commonly suffers high transverse compressive loads. Another example is the design development of aircraft CFRP struts which showed that the overall tensile strength and stiffness of a strut are limited by the transverse compressive strength and stiffness of the CFRP wedge joints [1].

According to various works [2–5] transversal compression strength is determined by the matrix type and its adhesion to the fibres. Failure is due to a shear in the plane oriented at some angle to the load axis. According to Collings [1] and Auzukalns *et al.* [5] this angle is not equal to 45° owing to an increase of shear strength in the presence of compressive stresses transverse to the shear plane. The effect was described [5, 6] by the Coulomb equation

$$\tau_s = \tau_0 + K\sigma_2 \quad (1)$$

where τ_0 is the shear strength in the absence of transversal stresses, σ_2 the compression stress, and K a constant.

Experimental investigations show that in reality the effect of the transversal component of compressive stresses, σ_2, is essentially non-linear [7–11]. For this reason, nonlinear criteria (for example Hill, Tsai–Wu, or others [7, 9, 11]) should be used.

To characterize shear and transversal properties of a unidirectional composite it is desirable to measure the strength and stiffness at transversal tension and compression. Shear properties parallel to the fibres must also be determined. Shear properties transverse to the fibres, i.e. through the thickness of the unidirectional ply, were not of primary interest, and are not easy to measure. However, with increasing concern for free-edge delamination associated with induced interlaminar stresses, transversal shear strength, τ_t, can no longer be neglected. The problem is to measure τ_t. Usually in order to describe shear and transversal properties, one uses a single constant – short beam shear (parallel to the fibres) strength τ_0.The main advantage of this method is simplicity of testing and of sample preparation. Unfortunately, short beam shear also has several disadvantages. For example, it does not allow evaluation of the shear modulus. In addition, even at fixed beam length to thickness ratio the strength depends on its thickness and the loading roller diameter [12–14] due to stress concentration near the roller [13, 14].

As the failure mechanism at transversal compression and transversal shear is the same, Bazhenov *et al.* [6] attempted to evaluate composite transversal shear strength, τ_t, by means of transversal compression. The results were compared with the short beam shear method. Transversal shear strength calculated from compression tests was lower than the short beam shear (parallel) strength. There may be two reasons for this: (1) transversal shear strength is really lower than at parallel shear; (2) the use of Equation 1 leads to a significant underestimation of τ_0.

Thus, the aims of the present paper are: (1) to investigate the transversal compression fracture, and

0022–2461/91 $03.00 + .12

(2) to analyse the possibility of shear strength measurements by means of transversal compression.

2. Experimental procedure

Hot-setting EDT-10 and EKT epoxy resins were used as a matrix (EDT-10 is more plastic and has lower strength). The principal experiments were carried out using the EDT-10 matrix. As a reinforcement E-glass, different carbon (T 800, IM6, Soviet UKN 5000 and high modulus HM), aramid polyamidobenzimidazole (PABI) and polyphenilenterephtalamid (PPTA) fibres were used [15] (PPTA properties are analogous to that of Kevlar 49). In order to investigate the effect of carbon fibres surface treatment, UKN 5000 fibres with and without any treatment were used (properties of UKN 5000 are analogous to T 300 fibres).

Transversal compression strength was measured by two different methods: (1) compression of rods with rectangular cross-section; (2) axial compression of unidirectional (90°) tubes.

The rods with rectangular cross-section were manufactured by wet winding of fibre thread on a mandrel with rectangular (4 mm × 10 mm) cross-section. Inner side walls of the mandrels were polished to obtain smooth and parallel rod side surfaces after resin curing. The specimens were loaded on these surfaces. The reinforcement fraction in the rod, V_f, was varied from 25 to 70 vol %. The specimens of 15 mm length were cut from the rods.

The tubes were manufactured by thread winding on a cylindrical mandrel. Tube wall thickness was $\approx$ 1.5 mm, inner diameter 20 mm and gauge length 90 mm. As the fibre content in tubes could not be altered, it remained constant equal to 65 to 70 vol %.

The shear strength was measured by short beam shear (length to thickness ratio was 5) and by torsion of unidirectional tubes. The strength values obtained by both methods were compared. The beam and tube specimens were the same as for the transversal compression tests.

The pore content was changed by using alcohol–acetone solutions of EDT-10 epoxy resin with different solvent concentrations as a matrix. The reduction of resin content leads to an increase in porosity after the solvent has been evaporated. The porosity was changed in the range 1 to 15 vol %.

The samples were tested on an "Instron 1169" machine at upper claw velocity of 0.1 mm min^{-1}. The butt ends of the fractured samples were investigated using a Jeol scanning electron microscope (SEM) and by long-focal optical microscope.

3. Results

3.1. Stress–strain curves

Fig. 1 shows compression stress–strain curves for different composites. Comparing stress–strain ($\sigma^- - \varepsilon_t^-$) diagrams for GFRP tubes and rods (curves 7 and 8) we may conclude that their shape and strength do not depend on the test method. As manufacturing of tube specimens is a time-consuming procedure, it is the rods which were mainly tested. Owing to low OFRP,

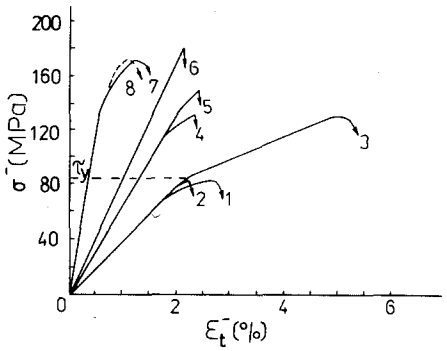

Figure 1 Compression stress, σ^-, plotted against strain, ε_t^-, for (1) PPTA/EDT, (2) PPTA/EKT, (3) PABI/EDT, (4) UKN-5000/EDT, (5) IM6/EDT, (6) T 800/EKT, (7, 8) glass/EDT, 1 to 7, rectangular cross-section specimens; 8, thin-walled tubes (90°).

transversal modulus failure of the tubes (1.5 mm wall thickness) is a result of buckling. Thus in the case of organic fibres, thicker tubes (2.5 to 3.0 mm) should be tested.

In the process of loading of FRP with plastic EDT matrix (PABI/EDT, PPTA/EDT and glass/EDT) at stresses equal to 75% to 85% ultimate strength, a non-linearity in the stress–strain curves shows up (Fig. 1, curves 1, 3, 7). Composites UKN 5000/EDT and IM 6/EDT also reveal non-linear deformation just before failure (curves 4, 5). On the contrary, deformation of CFRP on the base of brittle EKT matrix (T 800/EKT) is completely elastic up to failure (curve 6). Composite brittleness increases in the following order: PABI/EDT, PPTA/EDT, glass/EDT, carbon/EDT, carbon/EKT. PABI/EDT is more plastic not only in comparison with GFRP and CFRP but with PPTA/EDT as well. PABI/EDT reveals significant plastic straining and deformation strengthening. For this reason it will be characterized both by ultimate strength and yield stress.

Compression modulus E_t^-, was determined in accordance with the linear parts of the $\sigma^- - \varepsilon_t^-$ curves for tubes. E_t^- is equal to 3.6 to 4.2 GPa for both PABI/EDT and PPTA/EDT, 17 to 19 GPa for glass/EDT and 6.5 to 7.5 GPa for UKN 5000/EDT (V_f = 65 to 70 vol %). These values coincide with transversal tensile moduli determined by Lebedeva [16]. It must be noted that CFRP transversal modulus is significantly lower in comparison with GFRP. This result may be explained by high anisotropy and low transversal modulus of carbon fibres.

3.2. Transversal compression strength

Fig. 2 shows different composites compression strength, σ_t^-, plotted against fibre volume fraction, V_f. The pore volume fraction was < 1 vol %. GFRP strength does not depend on V_f (curve 2). The strength of OFRP and CFRP decreases slightly with increasing V_f. PABI/EDT strength is significantly higher than its yield stress. The cause for this is deformation strengthening and the formation of the specimen's barrel-like shape.

An increase in V_f leads to a reduction of PABI/EDT strength despite some yield limit groth. $\sigma^- - \varepsilon_t^-$ curves show that the strength decrease is due to a reduction

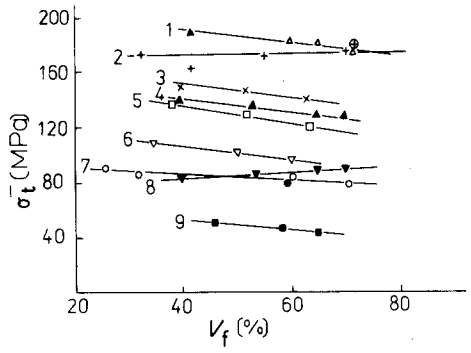

Figure 2 Transversal compression strength, σ_t^-, plotted against fibre volume fraction, V_f. 1, T 800/EKT; 2, glass/EDT, (⊕) tubes; 3, IM 6/EDT; 4, PABI/EDT; 5, UKN 5000/EDT; 6, HM/EKT; 7, (○) PPTA/EDT, (●) PPTA/EKT; 8, PABI/EDT yield stress; 9, untreated UKN 5000/EDT.

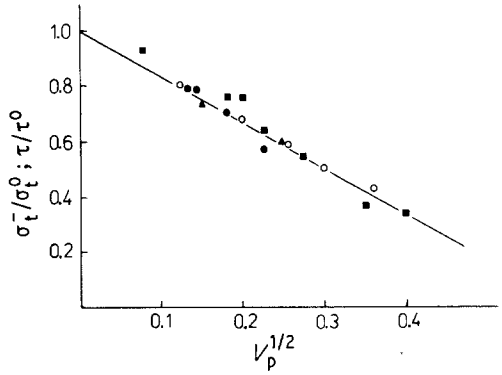

Figure 3 Normalized shear, τ, and transversal compression, σ_t^-, strengths plotted against square root of porosity, $V_p^{1/2}$. σ_t^0 and τ^0 are found by extrapolation of σ_t^- and τ to $V_p = 0$. (○) glass/EDT, short beam shear; (●) glass/EDT, compression; (■) UKN 5000/EDT, compression; (▲) T 800/EKT, compression.

of composite ultimate plastic strain and degree of strengthening.

Use of high-strength EKT matrix leads to an increase of CFRP compression strength (curves 1 and 3). According to some authors [16, 17], shear strength is also higher. Compression strength of composites reinforced by high-strength carbon fibres (T 800/EDT and IM6/EDT) is 5% to 10% higher compared with UKN 5000/EDT.

The strength of CFRP reinforced by high modulus (HM) fibres is quite low due to lower adhesion of fibres to the matrix [18]. Transversal strength of a composite reinforced by UKN 5000 fibres without any surface treatment is very low. We must also note the lower σ_t^- of CFRP in comparison with GFRP (curves 2, 3, 5). CFRP failure is brittle and it occurs immediately after a non-linearity in the $\sigma^- - \varepsilon_t^-$ curve appears. The reason may be somewhat lower adhesion to the matrix. It must be noted that σ_t^- plotted against V_f is never described by an uneven function as noted in [1].

The strength of PPTA FRP does not depend on matrix type (curve 7). This may be explained if it is supposed that OFRP shear strength is limited by aramid fibre properties due to lower fibre strength in comparison with that of the matrix.

3.3. Pores

It has been noted that different batches of specimens have a significant scatter of mean strength. An investigation of the cause has shown that low-strength specimens possess elevated porosity. As a result, the effect of pores on transversal and shear strength has been investigated.

Fig. 3 shows the normalized GFRP and CFRP shear and transversal compression strengths plotted against square root of porosity, $V_p^{1/2}$. Both dependencies are described by the single straight line with the slope equal to 1.65. This is possibly a result of the same failure mechanism both at shear and transversal compression.

3.4. Fracture

During loading in PABI/EDT, PPTA/EDT and glass/EDT at stresses equal to 75% to 85% of their strength there appears a non-linearity in stress–strain curves, which in PABI/EDT and PPTA/EDT is accompanied by the appearance of shear lines. The shear lines reveal composite intensive plastic deformation.

The fine structure of shear micro lines in OFRP was observed in SEM after failure. Both in PABI/EDT and PPTA/EDT at different SEM magnification, shears are observed at three different lengths: (1) shear macro cracks which are oriented at some angle (usually $\theta = 20°$ to $35°$) to the loading axis (Fig. 4a and b); (2) yield macro lines, 100 μm to 1 mm long, which are oriented exactly at angle 45° (Fig. 4b to d); (3) yield micro lines of 10 to 50 μm (fibre diameter) length (Fig. 4d to f).

Fig. 4e and f show that each thin yield macro line oriented exactly at 45° consists of micro lines which are oriented not only in this direction, but also in the perpendicular direction (−45°). This result seems very surprising. At any fibre content, micro and macro lines are oriented exactly at an angle of 45° (± 30′) to the loading axis.

The OFRP failure is a result of shear at some angle, θ, to the loading axis. Shear crack goes through the areas of elevated micro line concentration. In contrast with shear lines, the angle between the macro crack and the loading axis is not equal to 45°. The crack was born near one of the loading surfaces. This conclusion is based on the observation that the shear crack necessarily passes through one of the loading surfaces, and that the density of the shear lines near this surface is higher. The angle θ does not depend on the reinforcement content and is scattered over the range 35° to 41°. It must be noted that the scatter in θ is slightly lower in the case of one specimen batch.

The systems of shear micro lines in PABI/EDT and PPTA/EDT are quite different. In PABI/EDT shear micro lines are closer to one another as a result of higher plastic deformation. The most important is the difference in shear micro line shapes. If in PABI/EDT micro lines are straight (Fig. 4e), in PPTA/EDT they are shaped like segments of a circle 10 to 15 μm diameter (Fig. 4f). Therefore, it may be concluded that if in PABI/EDT shear lines pass through the matrix and the fibres, in PPTA/EDT the lines go round the fibres.

The failure of OFRP on the base of plastic EDT matrix is a result of shear in the plane, oriented at the angle of 35° to 41° to the loading axis (Figs 4a and b, 5a). If the matrix is elastic (PPTA/EKT) there are two types of fractured specimens (Fig. 5a and b). The first is totally analogous to that of PABI/EDT and PPTA/EDT. In the second type of specimen, the shear crack consists of two planes (Fig. 5b). On the butt-ends, two straight line segments of different length were observed. The shorter one (of 0.5 to 3 mm length) is near to the loading surface and the angle $\theta_1 = 35°$ to 41°. The longer one is oriented at $\theta_2 = 20°$ to 35°. Thus it is

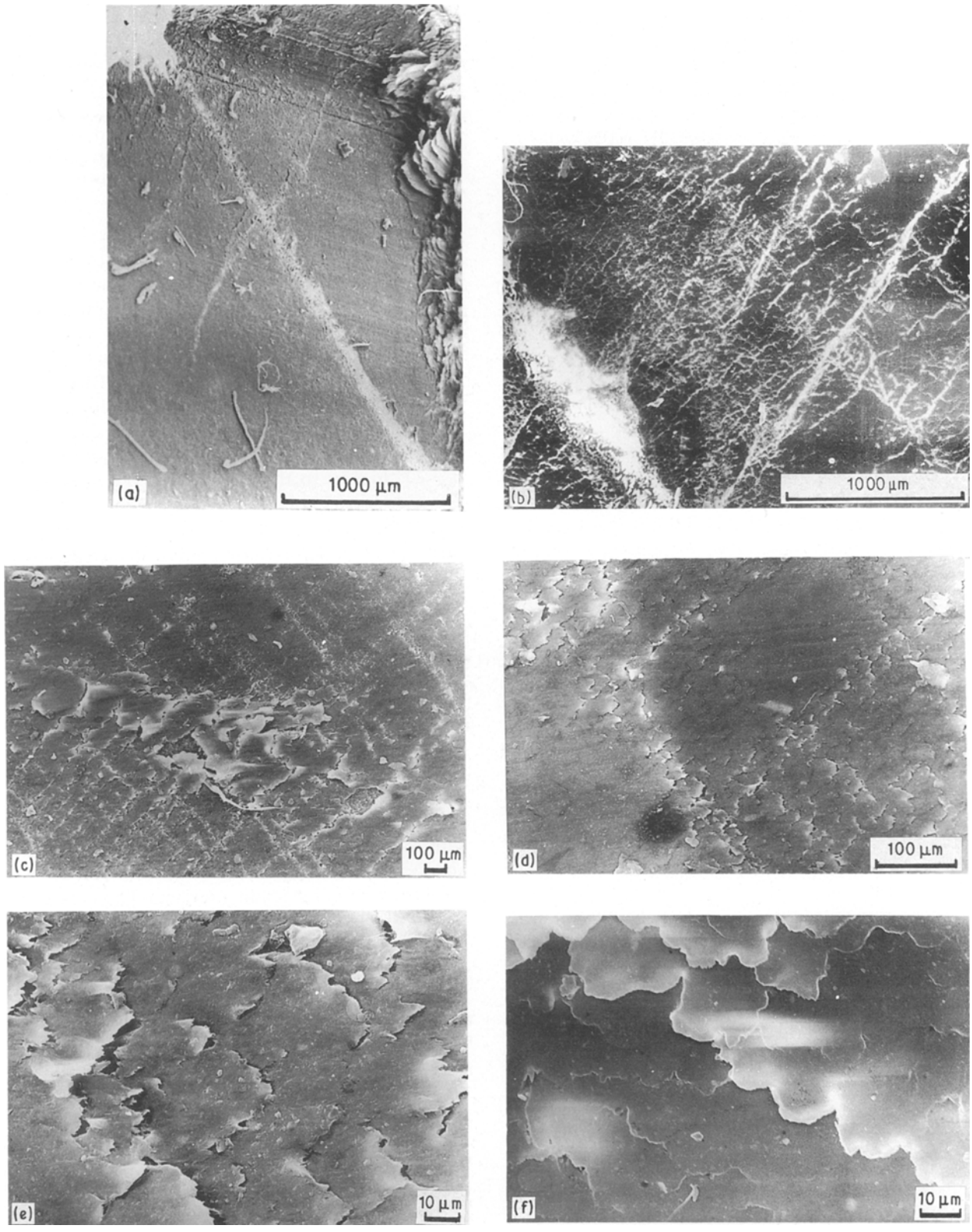

Figure 4 Photo of butt ends of fractured specimens. (a) Shear macro crack in PPTA/EDT. (b) Shear cracks and shear yield lines in PABI/EDT. (c, d, e) Yield macro and micro lines in PABI/EDT at different magnification. Black spot possesses to fix the position of the line (c, d). Each shear macro line (c) consists of a number of perpendicular micro lines (e). (f) Yield micro lines in PPTA/EDT. (g) Shear macro crack in UKN 5000/EDT. (h) Magnification of the region in which the shear crack (g) has appeared. The initial angle between the crack and the load direction 45°.

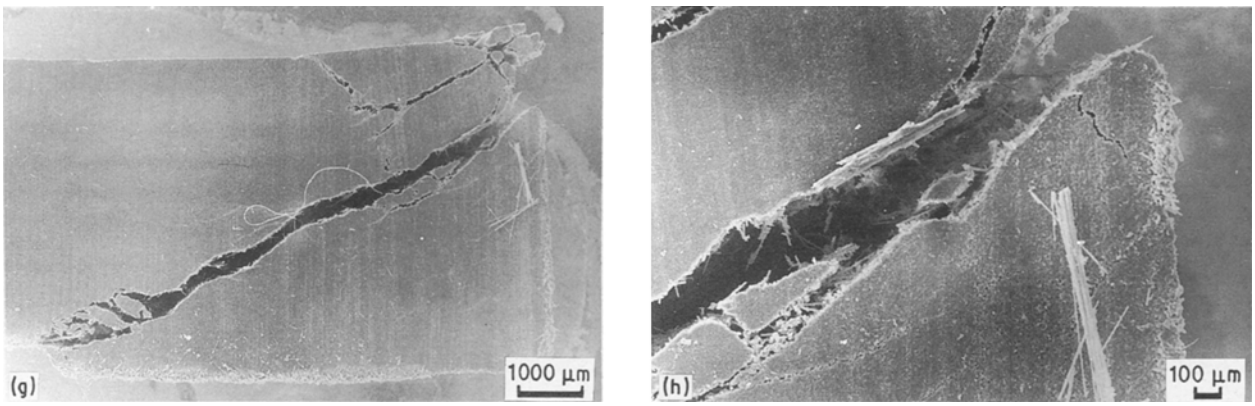

Figure 4 Continued

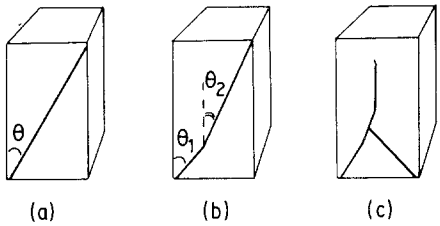

Figure 5 Composite failure modes under transversal compression. (a) Shear in the single plane, (b) turn of the shear crack, (c) several turns of the crack.

concluded that the shear crack appears near the loading surface and $\theta = 35°$ to $41°$. Later the crack turns along the loading direction.

The failure of GFRP is analogous to that of PPTA/EKT even when the plastic EDT matrix is used. Two types of fractured samples are observed (Fig. 5a and b). The shear crack initially appears at an angle of 35° to 45° to the loading axis.

The failure of CFRP is analogous to that of GFRP. The turning of the shear crack along the loading axis can also be observed. Instead of uneven turning, smooth turning is often observed. In addition, in CFRP secondary shear cracks intersecting with the primary one (Fig. 5c) can also be met. As a result the sample is divided into three or more parts. Fig. 4g and h show the turn of the initial direction of the crack.

4. Discussion

In composites with a plastic matrix base, during loading at some stress, a non-linearity in stress–strain curves appears (Fig. 1). The stress at which the non-linearity shows up depends on the fibre type. As a rule it is equal to 75% to 85% of the composite ultimate strength. When high strength EKT matrix was used the non-linearity was observed only in OFRP. As the EKT matrix is elastic, OFRP plastic deformation may be explained by plasticity of the fibres themselves.

Some increase in PABI/EDT yield stress with growth of V_f indicates that the matrix yield limit is lower than that of PABI fibres. The observation that micro lines pass through PABI and go around PPTA fibres is possibly a result of lower matrix adhesion to PPTA fibres. This presupposition is confirmed by significantly different transversal tensile strength of these composites (strength of PABI/EDT is 2 to 2.5 times higher in comparison with PPTA/EDT, Table I). Shear micro lines go around PPTA fibres as well as around the glass fibre, and pass through PABI fibres as through the epoxy matrix. As a result of extremely high PABI FRP transversal strength at equal fibre axial tensile properties, the axial strength of PABI FRP is $\approx 20\%$ higher [19, 20] due to the absence of longitudinal splitting under loading [20].

The directions of shear lines and shear macro cracks do not coincide. Thus in OFRP the plastic yield and the failure are connected but by different processes. The failure is a result of several micro lines amalgamation in a single macro crack. In the tip of a growing crack some secondary micro cracks may show up perpendicular to the initial crack. As a result the crack turns along the loading direction [21]. This failure mechanism is typical for rocks as well [21, 22].

In all composites the shear crack initially appears at an angle of $\theta_1 = 35°$ to $45°$ to the loading axis and later it may turn in the loading direction. At not very high microscope magnification the measured "mean" θ value may be significantly underestimated due to the turning of the crack. The decrease in the final angle, θ_f, and an increase in the turning angle, $\Delta\theta = \theta_i - \theta_f$ (θ_i and θ_f are initial and final angles) must be noted in the order PABI/EDT, PPTA/EKT, glass/EDT, carbon/EDT, carbon/EKT. Note that the composite brittleness increases in the same sequence. Thus it is concluded that the higher the composite plasticity, the lower is the turning angle. The reason for the crack turning is

TABLE I Mechanical characteristics of fibres tested

Fibre, matrix	Diameter (μm)	Modulus (GPa)	Strain (%)
UKN-5000	8.0	240	1.45
IM6	5.0	300	1.5
T-800	5.1	300	1.9
High modulus (HM)	8.0	560	0.3
E-glass	9.0	95	3.9
PPTA	13.0	130	3.0–3.5
PABI	13.0	120	4.0
EDT-10	–	2.6	5.7
EKT	–	2.6	2.9

possibly a transversal tensile stress in the crack tip [21, 22]. The lower the transversal tensile ultimate strength, the higher is the probability of crack turning due to a stress concentration in the growing crack tip. This supposition is confirmed by an increase of the stress intensity coefficient ratio, K_{IIc}/K_{Ic}, in CFRP ($\sim$ 6 to 8) compared with GFRP ($\sim$ 3 to 4) [23, 24]. An increase of K_{IIc}/K_{Ic} indicates that the danger of tensile cracking in the crack tip is growing.

An important question is whether the shear crack in composites reinforced with rigid fibres (GFRP and CFRP) appears initially as a yield line ($\theta = 45°$), or whether it is not connected with yield lines at all? To answer the question the point at which the crack appeared must be found. In some fractured specimens this was not possible. Sometimes it was seen that the crack appeared at an angle of 45° (Fig. 4h) but very often $\theta > 45°$. It is possible that the crack has turned very quickly and the result of the crack turning is seen. It is also possible that the crack emergence is not associated with the yield line. This question cannot yet be answered. To do so the fracture process near the instability point on stress–strain curve must be investigated.

Transversal compression and shear strengths plotted against fibre content show some strength decrease with V_f growth (GFRP is an exclusion). The effect may be explained by some growth of stress concentration near a rigid fibre. In accordance with Chamis [25] the increase in fibre content from 30 to 70 vol % leads to a growth of stress concentration from 2.2 to 2.4 (i.e. $\approx$ 10%). Approximately the same strength reduction is observed experimentally (Fig. 2).

Fig. 3 shows that the normalized shear and transversal compression strengths plotted against square root of porosity are described by a single straight line

$$\sigma_t^-/\sigma_t^0 = 1 - BV_p^{1/2}, \tau/\tau^0 = 1 - BV_p^{1/2} \quad (2)$$

where $B = 1.65$.

The shear strength dependence on pore content is often described by a linear function. As normally the scatter of experimental points is significant and V_p change is not high, the linear approximation fits the experiments in a satisfactory way. But when the porosity changes considerably, the non-linear character of the curve can be clearly seen.

Optical investigation of pores in GFRP shows that their shape is cylindrical with orientation along the fibre axis. To explain Equation 2, suppose that the cylindrical pores are arranged regularly (Fig. 6). It is natural to suppose that the shear crack grows through the plane in which a cross-section of the pores is maximum (plane A, Fig. 6). The pores part in this plane is equal to $\alpha = (4V_p/\pi)^{1/2}$. As the shear strength is proportional to the material cross-section in this plane, the following equation must be valid

$$\tau/\tau^0 = 1 - \alpha = 1 - (4/\pi)^{1/2} V_p^{1/2} \quad (3)$$

This equation coincides with Equation 2 if $B = (4/V_p)^{1/2} \approx 1.2$. A square root function is observed experimentally. In addition, the experimental B value (1.65) is very close to its theoretical value 1.2. Physically, Equation 2 is analogous to the Nicolais–Narkis

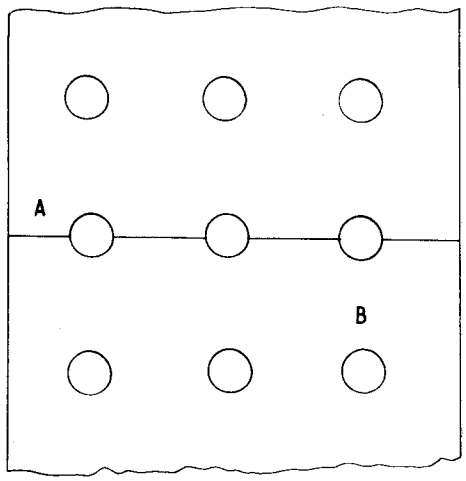

Figure 6 Model of composite with regularly arranged pores. A, crack plane; B, homogeneous composite.

equation [26] which describes the shear yield stress of the particle-filled composite (in the case of particles the power index is equal to 2/3). Owing to non-linear dependence of strength on V_p pores lead to a very abrupt reduction of shear and compression strength. For example, 1 and 4 vol % pores result in 16.5% and 33% reduction.

4.1. Transversal compression–shear strength correlation

To account for the effect of transversal to shear plane compression, the non-linear Tsai–Hanh criterion [7, 8, 11] was used

$$\frac{\sigma_2^2}{\sigma_t^+ \sigma_t^-} + \frac{\tau_s^2}{\tau_0^2} - \left(\frac{1}{\sigma_t^+} - \frac{1}{\sigma_t^-}\right)\sigma_2 = 1 \quad (4)$$

where σ_2 and τ_s are compression and shear stresses; σ_t^+, σ_t^- and τ_0 are strengths at "pure" transversal tension, compression and shear.

Typical shear strength plots against transversal stress σ_2 are shown in Fig. 7. Experimental data may be found for example in [8, 10]. For all composites (OFRP, CFRP and GFRP) $\tau_s(\sigma_2)$ plots have a maximum at $\tau_s/\sigma_2 = 1.0$ to 1.4. At the maximum point the derivative $d\tau_s/d\sigma_2 = 0$. As a result near the maximum the shear strength, τ_s, practically does not depend on the compressive stress, σ_2, and in this area we can consider $\tau_s = K\tau_0$ where K is the ratio of the maximum shear strength to τ_0.

If the external compressive stress is equal to σ_c, the projection of the stress on some plane oriented at an

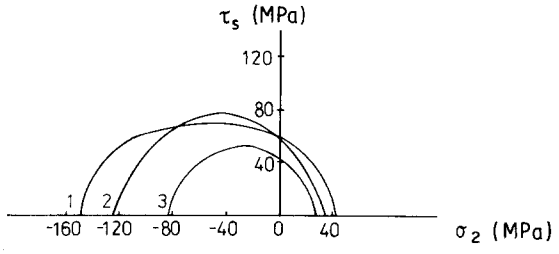

Figure 7 Shear strength, τ_s, plotted against transversal stress, σ_2. 1, GFRP; 2, CFRP; 3, OFRP.

angle θ to the loading axis (i.e. shear component of the external stress) is equal to

$$\tau_s = \tfrac{1}{2}\sigma_e \sin 2\theta \quad (5)$$

Analogously, the compressive component of the external stress is equal to

$$\sigma_2 = \sigma_e \sin^2\theta \quad (6)$$

Because in the investigated composites the crack appears at the angle θ = 35° to 45°, the τ_s/σ_2 ratio according to Equations 5 and 6 is equal to 1.0 to 1.50. This is the maximum region in Fig. 7, and in this area it is considered that $\tau_s \simeq K\tau_0$. In accordance with Fig. 7 the empirical K value is equal to 1.15 to 1.20 for OFRP, GFRP and CFRP. Consequently, the strength at "clear" shear may be calculated from the following equation

$$\tau_0 = \sigma_t^- \sin 2\theta/2K \quad (7)$$

where K = 1.15 to 1.20, and θ is the initial angle between the shear plane and the loading axis.

Shear strengths calculated in accordance with Equation 7 in practice coincide with the experimental

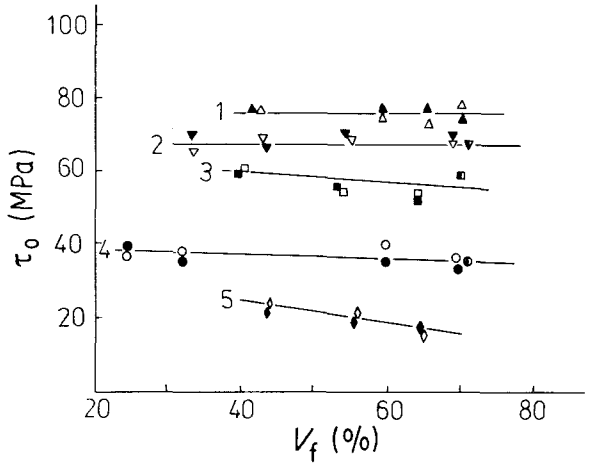

Figure 8 Shear strength, τ_0, plotted against fibre volume fraction, V_f. 1, T800/EKT, (△) short beam shear, (▲) transversal compression, calculation in accordance with Equation 7. 2, glass/EDT, (▽) shear, (▼) transversal compression, (▼) tubes. 3, UKN 5000/EDT, (□) shear, (■) transversal compression, (◧) tubes; 4, PPTA/EDT; (○) shear, (●) transversal compression, (◐) tubes; 5, untreated UKN 5000/EDT, (◇) shear, (◆) transversal compression.

ones (Fig. 8 and Table II). The only exclusion is PABI/EDT due to deformation strengthening and formation of a "barrel" which changes the initial cross-section of the specimen.

As sin 2θ is very close to 1.0 (0.91 to 1.00 in the range θ = 35° to 45°), Equation 5 may be rewritten into a very simple equation

$$\tau_0 = \sigma_t^-/M \quad (6)$$

where M = 2.3 to 2.4.

In our experiments, the empirical M coefficient is equal to 2.1 to 2.2 for CFRP, 2.6 to 2.8 for GFRP and ≃ 2.2 for PPTA FRP. M may also be evaluated as shown previously [8–10, 27–35]. Transversal compression strength in these works was measured by means of compressing rectangular cross-section rods and according to ITTRI and Celaneese methods which are used for axial compression strength measurements. Shear strength was measured by the Iosipescu method, by tube torsion (90°) and by tension of specimens with (± 45°) layers. For GFRP, M = 2.2 to 2.6 [9, 10, 28, 33], for OFRP M = 2.0 to 2.8 [27, 28, 31, 32] and for CFRP, M = 2.0 to 2.8 [8, 29, 30, 34, 35]. Thus it is concluded that M does not significantly depend on the fibre type and the test method. Of course the scatter in M may be due to errors in τ_0 and σ_t^- measurements. Therefore the shear strength can be evaluated if M = 2.4.

Thus allowing for the non-linear effect of transversal stress the results turned out even more simple in comparison with linear Coulomb Equation 1.

Coincidence of the calculated and experimental τ_0 values is very good (Fig. 8). Calculations were carried out using transversal compression strength which is determined by shear which was transversal to fibres while experimental measurements were carried out at parallel shear (thin-walled tubes and short beam shear). The dependencies of the calculated and experimental shear strengths on V_f are completely analogous.

Consequently we may conclude that transversal compression strength, and shear strengths in directions parallel and transversal to the fibre direction are very close composite characteristics. As a consequence there is no need for special measurements of transversal shear properties.

TABLE II Transversal and shear properties of composites

FRP[a]	σ_t^- (MPa)	σ_t^+ (MPa)[b]	τ_0 (MPa)[c]	τ_0 (MPa)[d]	τ_0 (MPa)[e]
UKN/EDT	122	28	54	58	52
UKN/EDT[f]	44	–	17	–	19
IM6/EDT	137	–	57	–	–
T-800/EKT	180	30	78	79	75
HM/EKT	98	–	40	–	–
Glass/EDT	170	55	67	68	69
PPTA/EDT	80	12	38	35	35
PPTA/EKT	79	–	37	35	34
PABI/EDT	128	26	38	37	–

[a] V_f = 65 to 70 vol %.
[b] Tube (90°) samples.
[c] Short beam shear.
[d] Tubes (90°).
[e] Shear strength calculated in accordance with Equation 1.
[f] UKN-5000 fibres without surface treatment.

5. Conclusions

1. Transversal compression failure is due to shear in plane oriented at some angle to the load axis. Shear cracks appear initially at the angle of 35° to 41° to the load direction. In GFRP and CFRP the crack turns along the fibre direction.

2. As the failure mechanism at transversal compression and shear is the same, transversal compression testing may be used to measure transversal shear strength.

3. GFRP shear and transversal compression strengths do not depend on fibre content, V_f. The strength of OFRP and CFRP is slightly reduced with an increase in V_f.

4. During loading in PABI/EDT, PPTA/EDT and glass/EDT at stresses equal 75% to 85% of their ultimate strength, there appears a non-linearity in the stress–strain curves, which in PABI/EDT and PPTA/EDT is accompanied by the appearance of shear lines.

5. Normalized shear and transversal compression strengths plotted against the square root of pore content are described by a single straight line.

References

1. T. A. COLLINGS, *Composites* **5** (1974) 108.
2. S. V. NAYES and B. H. JONES, in "Proceedings of AIAA/ASME 9th Structural Dynamics and Materials Conference', Palm Springs, California, April 1968, Paper N 68–336.
3. A. PUCK and W. SCHNEIDER, *Plastics and Polymers* **37** (1969) 33.
4. L. L. CLEMENS and R. L. MOORE, *Composites* **9** (1978) 93.
5. J. B. AUZUKALNS, F. J. BULAVS and G. M. GUNIAEV, *Polym. Mech.* (1973) 29, NI.
6. S. L. BAZHENOV, V. V. KOZEY, A. A. BERLIN, A. M. KUPERMAN, E. S. ZELENSKII and O. V. LEBEDEVA, *Dokl. Akad. Nauk* **303** (1988) 1155.
7. E. M. WU, in "Mechanics of Composite Materials", edited by G. P. Sendecky (Academic Press, New York, London, 1974) Ch. 9, p. 353.
8. K. IKEGAMI, in "Carbon Fibres", edited by S. Simamura (Mir, Moscow, 1987) p. 185 (Translated from Japanese to Russian).
9. H. T. HANH, J. B. ERIKSON and S. B. TSAI, in "Strength and Fracture of Composite Materials", edited by G. C. Sih and V. P. Tamuzh (Zinatne, Riga, 1983) p. 259 (in Russian).
10. A. M. SKUDRA and F. J. BULAVS, in "Strength of Reinforced Plastics" (Khimia, Moscow, 1982) p. 151 (in Russian).
11. R. ROWLANDS, in "Inelastic Behaviour of Composite Materials", edited by C. T. Herakovich (ASME, New York, 1975) p. 140.
12. B. ROSEN and N. DOW, in "Fracture of Nonmetals and Composites", edited by H. Liebowitz (Academic Press, New York, London, 1972) p. 301.
13. J. M. TARNOPOLSKII and T. J. KINZIS, "Methods of Reinforced Plastics Testing" (Khimia, Moscow, 1981) p. 263 (in Russian).
14. S. M. WHITNEY and C. E. BROWNING, *Exp. Mech.* **25** (1985) 294.
15. G. A. BUDNITSKII, *J. USSR Mendeleev's Chem. Soc.* **34** (1989) 438.
16. O. V. LEBEDEVA, Dokt. Dissert., Institute of Chemical Physics, USSR Academy of Science, Moscow, 1987.
17. A. M. KUPERMAN, N. A. SNEGIREVA, V. V. KOZEY, L. V. PUCHKOV, S. L. BAZHENOV and E. S. ZELENSKII, in "Reinforced Plastics-89" (Karlovi Vary, Czechoslovakia, 1989) p. 144.
18. I. L. KALNIN and H. JAGER, in "Carbon Fibres and Their Composites", edited by E. Fitzer (Springer–Verlag, Berlin, 1985, 1986) p. 83.
19. V. N. KUZMIN, A. S. ANDREEV and I. P. DOBROVOLSKAJA, *Compos. Mech.* (1985) 736.
20. E. F. KHARCHENKO, S. L. BAZHENOV, A. A. BERLIN and A. A. KULKOV, *ibid.* (1988) 67.
21. L. OBERT, in "Fracture of Nonmetals and Composites", edited by H. Liebowitz (Academic Press, New York, London, 1972) p. 60.
22. H. HORII, S. NEMAT-NASSER, *J. Geophys. Res.* **90** (1985) B4, 3105.
23. E. M. WU, in "Fracture and Fatigue", edited by L. S. Broutman (Academic Press, New York, London, 1974) p. 206.
24. R. A. SURF and B. B. PIPES, *Carbon Reinf. Epoxy Syst.* **13**(5) (1984) 52.
25. S. S. CHAMIS in "Fracture and Fatigue", edited by L. S. Broutman (Academic Press, New York, London, 1974) p. 106.
26. L. NICOLAIS and M. NARKIS, *Polymer Engng Sci.* **11** (1971) 194.
27. E. A. SOKOLOV, *Compos. Mech.* (1979) 799.
28. V. G. PEREVOZCHIKOV, V. A. LIMONOV, V. D. PROTASOV and V. P. TAMUZH, *ibid.* (1988) 845.
29. C. POON, P. SCOTT and S. LEE, *Polym. Compos.* **9** (1988) 318.
30. J. MATSUI, S. NAMURA and Y. ISHII, *J. Jpn Soc. Compos. Mater.* **12** (1986) N6, 11.
31. R. D. MAKSIMOV, E. Z. PLUME and V. V. PONOMAREV, *Compos. Mech.* (1984) 35.
32. V. P. TAMUZH and V. D. PROTASOV, in "Fracture of Composite Materials", edited by V. D. Protasov (Riga, Zinatne, 1987) p. 227.
33. S. W. MOORE and D. L. SURGEON, *Composites* **4** (1973) 34.
34. S. K. HA and G. S. SPRINGER, in "Proceedings of the ICCM-VI and ECCM-2", Vol. 4, London, 1987, edited by F. L. Matthews, N. C. R. Buskell, J. M. Hodgkinson and J. Morton (Elsevier Applied Science, London, 1987) p. 422.
35. S. LIFSHITZ, *J. Compos. Tech. Res.* **10** (1988) 100.

Received 8 February
and accepted 19 February 1990